Computers & Geosciences 49 (2012) 190–199

Contents lists available at SciVerse ScienceDirect

Computers & Geosciences

journal homepage: www.elsevier.com/locate/cageo

Load Love numbers and Green's functions for elastic Earth models PREM, iasp91, ak135, and modified models with refined crustal structure from Crust 2.0☆

Hansheng Wang [a,*], Longwei Xiang [a,b], Lulu Jia [a,b], Liming Jiang [a], Zhiyong Wang [c], Bo Hu [a,b], Peng Gao [a,b]

[a] State Key Laboratory of Geodesy and Earth's Dynamics, Institute of Geodesy and Geophysics, Chinese Academy of Sciences, Wuhan 430077, China
[b] Graduate University of Chinese Academy of Sciences, Beijing 100049, China
[c] Department of Surveying Engineering, Shandong University of Technology, Zibo 255049, China

ARTICLE INFO

Article history:
Received 29 October 2011
Received in revised form
26 June 2012
Accepted 27 June 2012
Available online 7 July 2012

Keywords:
Loading Love numbers
Green's function
PREM
iasp91 and ak135
Crust 2.0

ABSTRACT

Load Love numbers and Green's functions are computed for elastic Earth models PREM, iasp91 and ak135, and their modified models with refined crustal structure from Crust 2.0. It is found that the differences of results between iasp91 or ak135 and PREM, and the effects of refinement of crustal structure are significant for the Love numbers of degrees from around 200 to very high numbers, and for the Green's functions in the near-field. The results of the models given in this paper are applicable to the studies related to loading processes (present surface mass transport as measured by GRACE and GPS, ocean tide loading, etc.), making it possible to use different models or assess the uncertainties of solutions of the loading problems under investigation. In order to ensure the stability of the solutions for degrees larger than 360 (or when the resolution is less than 55 km), a variable transformation on the solution vector is used in this paper and proved to work effectively.

© 2012 Elsevier Ltd. All rights reserved.

1. Introduction

Since both load Love numbers (LLNs) and load Green's functions (LGFs) are dependent strongly upon the *P*-wave velocity V_P, *S*-wave velocity V_S and density ρ for a spherically-symmetric non-rotating elastic isotropic (SNREI) Earth model, the numerical results must be updated along with the development of new Earth models with new data constraints.

PREM Earth model (Dziewonski and Anderson, 1981) used the data of body wave travel times and the periods of normal modes from years 1964 to 1975 collected by the International Seismological Centre (ISC). For Earth model iasp91 (Kennett and Engdahl, 1991), the data of body waves used were extended to 1987 and for the follow-on ak135 model (Kennett et al., 1995), the data of *P* wave were extended to 1991. The largest differences of elastic structures between iasp91/ak135 and PREM can be found in the shallow part of the Earth (Figs. 1 and 2). Especially, PREM includes a discontinuity at depth 220 km which iasp91 and ak135 do not support. The differences between model iasp91 and ak135 are usually very small except for the *S*-wave velocity within 50 km depth. However, although the subsequent Earth models iasp91 and ak135 were already produced, the model PREM has been widely used to investigate the loading responses to ocean tide, terrestrial water change, ice-melting, and last deglaciation since it was proposed in 1981 (e.g., Han and Wahr, 1995; Wang et al., 1996; Guo et al., 2001; Van Dam et al., 2002). In spite of the changes of elastic structures of the two new models compared with PREM, they have been neglected for a long time in loading process modeling. Recently, Na and Baek (2011) presented the results of LNNs and LGFs for iasp91 model. However, the highest degree is limited to 10,000.

Moreover, although Crust 2.0 (Laske et al., 2012) has been producing new results of crustal elastic structure with increasing resolution in depth direction, showing large gaps in comparison with the above three models (Fig. 2), it has usually not been included in the Earth model for the modeling of loading process.

Accordingly, the aim of this paper is to compute the LLNs and LGFs for the three representative Earth models and the modified models with crust substituted by the globally-averaged Crust 2.0, and to investigate how the differences in Earth's elastic structures affect the numerical results.

For the computation of LLNs and LGFs, some previous works have been taken into account the lateral heterogeneity (e.g., Plag et al., 1996) and the anisotropy of mantle (e.g., Pagiatakis, 1990) which are, however, not the topics of this paper.

2. Numerical method

LGF is defined as the surface deformation of the Earth due to a point load on the Earth's surface (Longman, 1962, 1963), and can

☆The data is available from server at http://www.iamg.org/CGEditor/index.htm.

* Corresponding author. Tel.: +86 276881341; fax: +86 278673841.
E-mail address: whs@asch.whigg.ac.cn (H. Wang).

0098-3004/$ - see front matter © 2012 Elsevier Ltd. All rights reserved.
http://dx.doi.org/10.1016/j.cageo.2012.06.022

be conveniently expressed through three LLNs (h_n, l_n, k_n) (Farrell, 1972). For an arbitrarily distributed mass load on the surface, the resultant responses can be computed by convoluting the related LGFs and the load (Peltier and Andrews, 1976; Wu and Peltier, 1982). Thus, in this paper we focus on the computation of LLNs and LGFs for the Earth models mentioned above. The fundamental methodology related to the computations can be found in previous works (e.g., Longman, 1962; Farrell, 1972; Wu and Peltier, 1982). As in Wu and Peltier (1982), one can find how the partial differential field equations are transformed into ordinary differential equations (ODEs, Eq. (8)), and how the ODEs are solved by the Runge–Kutta method using boundary conditions at the core–mantle boundary (CMB) (Eq. (48)) and on the Earth's surface (Eq. (11)), then we compute the LLNs (Eq. (12)) and LGFs (Farell, 1972) as also outlined in Appendix A and Appendix B. However, for higher degrees, the computation can be subjected to numerical overflow or instability. In order to ensure the stability when solving the ODEs for higher degrees, Riva and Vermeersen (2002) developed an approximate approach and Wang et al. (1996) proposed a variable transformation approach. In this paper, we use the latter one since it is not based on any assumption. It is noted that Wang et al. (1996) just mentioned the transformation of the ODEs but did not give the results transformed for the boundary conditions at CMB and on the Earth's surface, and the final formulas for LLNs. Therefore, in the following, we thoroughly formulate the related procedures for the transformation approach.

Since for an incompressible homogeneous SNREI model, as in Wu and Peltier (1982), the solution vector $Y=(y_1, y_2, y_3, y_4, y_5, y_6)^T$ of the ODEs (Eq. (8)) was found to have a r^n factor (e.g., Eq. (30)), for a compressible layered SNREI model considered in this paper, thus we can define a new solution vector Z transformed from Y in the following:

$$Y = r^n Z. \tag{1}$$

The numerical computation of Z would not overflow and would be stable. Inserting Eq. (1) into the ODEs (Eq. (8)) and surface boundary condition (Eq. (11)), we have new ODEs

$$\frac{dZ}{dr} = \left(A - \frac{n}{r}E\right)Z, \tag{2}$$

and new surface boundary condition,

$$\begin{cases} z_3(a) = r^{-n} y_3(a) \\ z_4(a) = r^{-n} y_4(a) \\ z_6(a) = r^{-n} y_6(a) \end{cases}, \tag{3}$$

where E is the unit matrix, and $[y_3(a), y_4(a), y_6(a)]$ are given by surface boundary condition (Eq. (11)). Since the same factor is used for the transformation of all the elements of the solution vector, the boundary condition at the CMB (Eq. (48)) is unchanged. However the solution (Eq. (49)) on the surface of a small uniform sphere ($r=\delta r$) located at the center of the core is transformed into $[1, 2(n-1)\delta r^{-1}]^T$ as initial value for integrating ODEs in the core (Eq. (8)).

Using the new solution vector Z, the corresponding LLNs computed as in Eqs. (A1) for $n>1$ can be written as:

$$\begin{bmatrix} h_n \\ l_n \\ k_n+1 \end{bmatrix} = \frac{g_0(a)}{\Phi_{2n}(a)} \begin{bmatrix} z_{11}(a) & z_{12}(a) & z_{13}(a) \\ z_{21}(a) & z_{22}(a) & z_{23}(a) \\ -z_{51}(a)/g_0 & -z_{52}(a)/g_0 & -z_{53}(a)/g_0 \end{bmatrix}$$

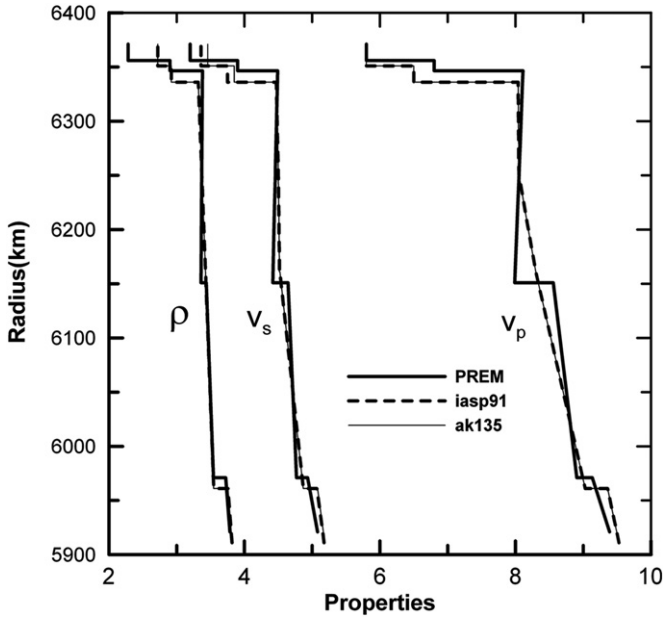

Fig. 1. Comparison of the density and velocity within 400 km depth among PREM, iasp91, and ak135. ρ—density; V_P—P-wave velocity and V_S–S-wave velocity.

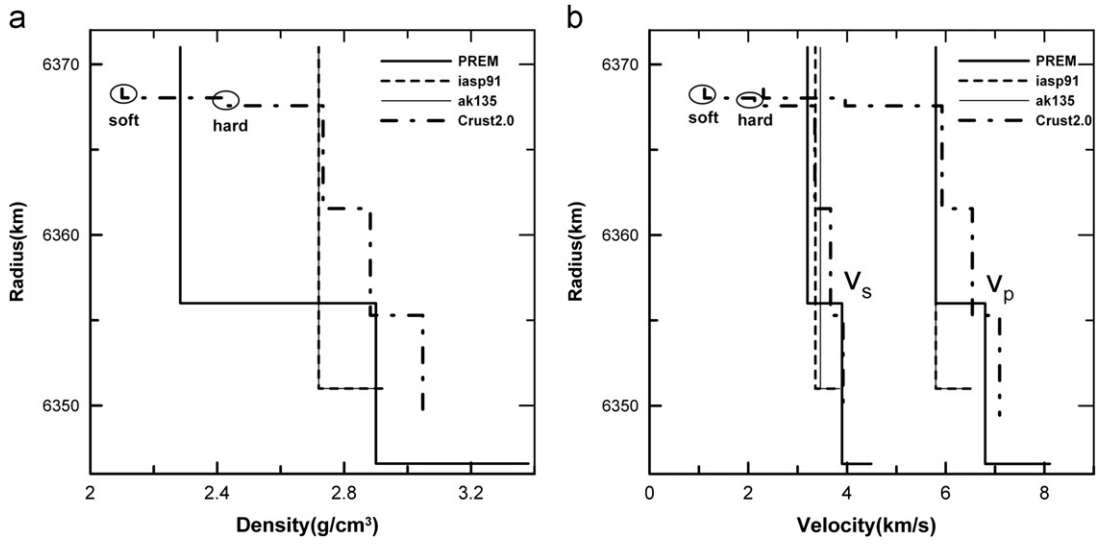

Fig. 2. Comparison of the density (a) and velocity (b) within 20 km depth among PREM, iasp91, ak135 and globally-averaged Crust 2.0. Soft/hard denotes soft/hard sediment with thicknesses of 0.52 km/0.46 km.

Download English Version:

https://daneshyari.com/en/article/507422

Download Persian Version:

https://daneshyari.com/article/507422

Daneshyari.com